



Hydrodynamic cavitation induced fabrication of soy protein isolate–polyphenol complexes: Structural and functional properties

Fengyan Wei^a, Xian'e Ren^{a,b}, Yongchun Huang^{a,b}, Ning Hua^a, Yuting Wu^a, Feng Yang^{a,b,*}

^a School of Biological and Chemical Engineering, Guangxi University of Science and Technology, Guangxi Key Laboratory of Green Processing of Sugar Resources, Key Laboratory for Processing of Sugar Resources of Guangxi Higher Education Institutes, Liuzhou, 545006, China

^b Guangxi Liuzhou Luosifen Research Center of Engineering Technology, Liuzhou, 545006, China

ARTICLE INFO

Handling Editor: Dr. Maria Corradini

Keywords:

Hydrodynamic cavitation

Soy protein isolate

Polyphenol

Structure

Functionality

ABSTRACT

The combination of polyphenols and protein can improve the functional characteristics of protein. How to effectively promote the binding of polyphenols to protein is still a difficult topic. In this study, hydrodynamic cavitation (HC) was used to induce the fabrication of complexes between soy protein isolate (SPI) and different polyphenols (tannic acid (TA), chlorogenic acid (CGA), ferulic acid (FA), caffeic acid (CA), and gallic acid (GA)). The effect of HC on the interaction between polyphenols and SPI was investigated, and the structural and functional properties of the formed complexes were characterized. The results showed that HC treatment led to SPI structure stretching, which increased the binding level of polyphenols, especially that of TA (increased from $35.08 \pm 0.73\%$ to $66.42 \pm 1.35\%$). The increase in ultraviolet–visible absorption intensity and quenching of fluorescence intensity confirmed that HC enhanced the interaction between polyphenols and protein. HC treatment reduced the contents of free sulfhydryl and amino groups in SPI–polyphenol complexes and altered their Fourier transform infrared spectroscopy, indicating that HC treatment promoted the formation of C–N and C–S bonds between SPI and polyphenols. Circular dichroism spectroscopy indicated that HC treatment altered the secondary structure of SPI–polyphenol complexes, inducing an increase in α -helix and random coil contents and a decrease in β -sheet content. Regarding functional properties, HC treatment improved the emulsification and antioxidant activity of SPI–polyphenol complexes. Therefore, HC is an effective technique for promoting the binding of polyphenols to protein.

1. Introduction

With the growing market demand for functional foods, scholars are focusing on improving the functional properties and physiological activities of protein by studying their interactions with small molecular substances. Polyphenols are small molecules comprising aromatic rings and polyhydroxyl groups. Polyphenols exert various physiological functions, such as antioxidation, free radical scavenging, antiallergy, anticancer, hypoglycemic, and antiaging effects (Dini and Grumetto, 2022), and they are widely used in the development of functional foods.

Previous studies have shown that protein interact with polyphenols covalently and noncovalently (Li et al., 2021c). Noncovalent interactions involve protein side chain residues (e.g., hydrophobic groups, $-\text{NH}_2$, and $-\text{OH}$) with hydroxyl groups, benzene rings, and carbonyl groups of polyphenols interacting through mechanisms including hydrogen bonding, hydrophobic interactions, electrostatic interactions, and van der Waals forces. Additionally, covalent interactions occur when the phenolic hydroxyl groups of polyphenols are easily oxidized to quinone structures under oxygen, free radical, and alkaline conditions. Then, the quinone structure combines with the nucleophilic groups of

Abbreviations: HC, Hydrodynamic cavitation; SPI, soy protein isolate; TA, tannic acid; CGA, chlorogenic acid; FA, ferulic acid; CA, caffeic acid; GA, gallic acid; EGCG, epigallocatechin gallate; DTNB, 5,5-dithiobis-(2-nitrobenzoic acid); 1,8-ANS, 8-aniline-1-naphthalene sulfonic acid; OPA, ortho-phthaldialdehyde; DPPH, 1,1-diphenyl-2-pyrroldinohydrazine; ABTS⁺, 2,2'-azino-bis(3-ethylbenzothiazoline-6-sulfonic acid) diammonium salt; SDS, sodium dodecyl sulfate; H_0 , surface hydrophobicity; FRAP, ferric ion reducing antioxidant power; EAI, emulsifying activity index; ESI, emulsifying stability index; λ_{max} , maximum fluorescence emission wavelength.

* Corresponding author. School of Biological and Chemical Engineering, Guangxi University of Science and Technology, Guangxi Key Laboratory of Green Processing of Sugar Resources, Key Laboratory for Processing of Sugar Resources of Guangxi Higher Education Institutes, Liuzhou, 545006, China.

E-mail addresses: weifengyan2022@163.com (F. Wei), renxiane2014@126.com (X. Ren), huangyc@yeah.net (Y. Huang), 13057171823@163.com (N. Hua), wyt_be_happy@163.com (Y. Wu), yfyangfeng@hotmail.com (F. Yang).

<https://doi.org/10.1016/j.crfs.2024.100969>

Received 19 September 2024; Received in revised form 21 December 2024; Accepted 31 December 2024

Available online 2 January 2025

2665-9271/© 2025 The Authors. Published by Elsevier B.V. This is an open access article under the CC BY-NC-ND license (<http://creativecommons.org/licenses/by-nc-nd/4.0/>).

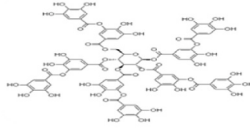
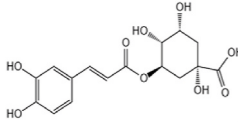
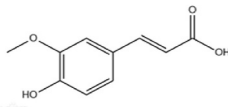
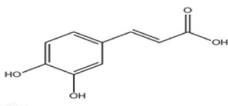
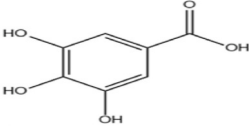
the protein side chain, such as through C–N and C–S bonds. These interactions can alter the protein structure, give protein antioxidant properties, and improve other functional properties of the protein. For example, tea polyphenol and egg white protein formed a complex at neutral (pH 7.0) that improved the emulsification of egg white protein (Sun et al., 2022). The covalent combination of casein and quercetin changed the secondary structure of casein and improved the solubility, foam activity, emulsification activity, and antioxidant activity of casein (Ke et al., 2023). In addition, protein-polyphenol complexes also played a significant role in enhancing the functional properties and quality of food (Kim et al., 2024).

The molecular weight, number and location of hydroxyl groups of polyphenols are internal factors affecting their interactions with protein (Kim et al., 2024). For example, among the three polyphenols of epigallocatechin gallate (EGCG), chlorogenic acid (CGA), and caffeic acid (CA), the complex formed by the high molecular weight EGCG and protein had a high binding equivalent (Meng and Li, 2021). Among the three polyphenols (quercetin, rutin, and ellagic acid), quercetin, which had more phenolic hydroxyl groups, had the highest binding rate with lentil protein isolate (Parolia et al., 2022). However, most recent studies focused on interactions between different flavonoid polyphenols and protein, and there are few studies on other polyphenols (such as phenolic acids, tannins, and stilbenes). Therefore, five nonflavonoid polyphenols (tannic acid (TA), CGA, ferulic acid (FA), CA, and gallic acid (GA)) were studied here. Among them, TA has dihydroxyphenol and trihydroxyphenol structures and can interact with protein as a molecular cross-linking agent (Hu et al., 2023). CGA, FA, and CA are phenolic acids containing hydroxycinnamic acid, whereas GA is a phenolic acid containing hydroxybenzoic acid; the former is more likely to be deprotonated under neutral conditions (Li et al., 2021). Moreover, there are substantial differences in the molecular weight, number of hydroxyl groups, and position of the hydroxyl groups among the five polyphenols (Table 1). Hence, there may be differences in the main driving forces of their interactions with protein, which affect protein structure

differently.

The rigid structure of protein provides them with high stability and resistance to deformation in their native state, which significantly limits the exposure of binding sites within the protein interior (Chen et al., 2024b). Consequently, it obstructs the pathways for the binding of polyphenols to protein, thereby constraining their interaction. Therefore, people are constantly trying to explore new and more effective processing technologies to prepare protein-polyphenols complexes. Ultrasound has been shown to generate shear force, turbulence, and microjets that might destroy protein structure, increase the protein-specific surface area, and expose more binding sites, thus promoting interactions between protein and polyphenols (Liu et al., 2023b). In addition, the hydroxyl radicals generated by ultrasound not only attack protein to produce protein free radicals and promote covalent interaction between protein and polyphenols (Liu et al., 2023b), but also attack polyphenols and oxidize them into quinones, which then covalent interaction with the side chain groups of protein (Zheng et al., 2023). In addition, the shear force generated by high-pressure treatment destroys the protein structure and exposes the buried groups, improving the solubility and emulsification of tea polyphenol-*soybean protein complexes* (Chen et al., 2019). These studies showed that these new processing technologies could be applied to interactions between protein and polyphenols. Similarly, hydrodynamic cavitation (HC), a new processing technology, combines physical effects with chemical effects and has a cavitation effect similar to that of ultrasonic cavitation (Ren et al., 2020). In HC, when the liquid passes through the orifice plate, venturi tubes, impellers, or rotors, the cavitation effect is generated due to the sudden alteration of pressure or velocity to form bubbles. In the flow process, the bubbles expand and then break rapidly, resulting in high shear force, microjets, shock waves, and free radicals that cause or accelerate physical or chemical changes in substances (Yang et al., 2018). Furthermore, HC technology requires simple equipment, is easy to operate, conserves energy, and can be used for large-scale applications (Panda et al., 2020). Currently, the application of HC technology in

Table 1
Differences between various polyphenols.

Polyphenol	Relative molecular mass	Structural formula	Number of phenolic hydroxyl groups	Number of hydroxyl groups
TannicTA acid (TA)	1701.2		25	-
Chlorogenic acid (CGA)	354.3		2	3
Ferulic acid (FA)	194.2		1	-
Caffeic acid (CA)	180.2		2	-
Gallic acid (GA)	170.1		3	-

the field of protein modification is gradually increasing. For example, Yu et al. (2024) pointed that the hydroxyl radicals, hydrogen peroxide, and ozone generated during HC treatment participated in the modification of wheat gliadin. This process altered the secondary structure of wheat gliadin and its specific celiac-toxic peptides, thereby reducing the allergenicity. Patil et al. (2023) found that after HC treatment, casein underwent significant conformational changes and structural rearrangements, which enhanced its solubility, water-holding capacity, and in vitro digestibility. In addition, our group had also conducted numerous studies on protein modification using HC technology, demonstrating that HC treatment stretched the protein structure, exposed the internal buried groups, and interrupted interactions between protein, thus affecting the emulsification, solubility, and gel properties of protein (Ren et al., 2020; Xie et al., 2024; Yang et al., 2018). Therefore, it is speculated that HC technology can promote interactions between SPI and polyphenols and change the physicochemical and functional properties of protein–polyphenol complexes. However, so far, there have been few experimental studies on the application of HC technology in the interaction between protein and polyphenols.

The purpose of this study was to use HC technology to promote the interaction between SPI and different polyphenols to prepare protein–polyphenol complexes with excellent antioxidant and emulsifying properties. In order to study the mechanism of the effect of HC treatment on the interaction between protein and polyphenols, the contents of free sulfhydryl and amino groups were measured, and ultraviolet–visible spectroscopy, endogenous fluorescence spectroscopy, and Fourier transform infrared spectroscopy were analyzed. Surface hydrophobicity and Circular dichroism spectroscopy were also analyzed to characterize the structural properties of the prepared complexes. The obtained results would provide a theoretical basis for the application of HC technology in the preparation of protein–polyphenol complexes and broaden the development and application of SPI and polyphenols.

2. Materials and methods

2.1. Materials

SPI (purity >90% protein) was purchased from Shandong Yuwang Ecological Food Industrial Co., Ltd. (Shandong, China). TA, CGA, FA, CA, and GA (purity of 95, 95, 99, 98, and 99%, respectively), and 5,5-dithiobis-(2-nitrobenzoic acid) (DTNB) were purchased from Shanghai Aladdin Biochemical Technology Co., Ltd. (Shanghai, China). Dialysis bags (3500 Da, 44 mm) and 8-aniline-1-naphthalene sulfonic acid (1,8-ANS) were purchased from Shanghai Yuanye Bio-Technology Co., Ltd. (Shanghai, China). Folin-Ciocalteu's reagent, ortho-phthalaldehyde (OPA), 1,1-diphenyl-2-pyrrolidinohydrazine (DPPH·), and 2,2'-azino-bis(3-ethylbenzothiazoline-6-sulfonic acid) diammonium salt (ABTS⁺) were purchased from Shanghai Macklin Biochemical Technology Co., Ltd. (Shanghai, China). All other reagents used in the study were of analytical quality or better.

CA, and GA (purity of 95, 95, 99, 98, and 99%, respectively), and 5,5-dithiobis-(2-nitrobenzoic acid) (DTNB) were purchased from Shanghai Aladdin Biochemical Technology Co., Ltd. (Shanghai, China). Dialysis bags (3500 Da, 44 mm) and 8-aniline-1-naphthalene sulfonic acid (1,8-ANS) were purchased from Shanghai Yuanye Bio-Technology Co., Ltd. (Shanghai, China). Folin-Ciocalteu's reagent, ortho-phthalaldehyde (OPA), 1,1-diphenyl-2-pyrrolidinohydrazine (DPPH·), and 2,2'-azino-bis(3-ethylbenzothiazoline-6-sulfonic acid) diammonium salt (ABTS⁺) were purchased from Shanghai Macklin Biochemical Technology Co., Ltd. (Shanghai, China). All other reagents used in the study were of analytical quality or better.

2.2. Preparation of SPI–polyphenol complexes with or without HC treatment

The schematic of HC experimental device is shown in Fig. 1. The system consists of a centrifugal pump (550 W), a storage tank, a thermostatic bath, a single orifice plate (diameter 3 mm, thickness 20 mm), pressure gauges (P₁ and P₂, which are used to measure the fluid pressure upstream and downstream of the single orifice plate, respectively), control valves (V₁ and V₂, which are used to control the sample flow), a sample valve (V₃, which is used for sampling), and a pipeline. The sample solution in the storage tank circulates continuously with the assistance of the centrifugal pump. When the sample fluid flows through the orifice plate, the flow velocity will suddenly increase due to the pipe narrowing, causing rapid decrease in pressure of fluid. When the pressure is lower than the saturated vapor pressure of the fluid medium, cavitation bubbles will be formed. With the flow of the fluid, the pressure will further decrease, and the cavitation bubbles will increase continuously. When the fluid flows downstream of the orifice plate, the outlet pressure suddenly increases causing cavitation bubble collapses, accompanied by shock wave, shear force, microjet, free radicals, local high temperature and other cavitation phenomena.

SPI (5.0 g) was dissolved in 250 mL of deionized water and magnetically stirred for 2 h. TA, CGA, FA, CA, and GA (0.5 g each) were dissolved in 250 mL of 20 mM phosphate buffer (PBS, pH 7.0) separately. The SPI dispersion was mixed with polyphenol solution (at a volume ratio of 1:1), and then the pH was adjusted to 7.0 with 2 M NaOH. For the sample subjected to HC treatment, the mixed solution was poured into the storage tank. The switch of the thermostatic bath

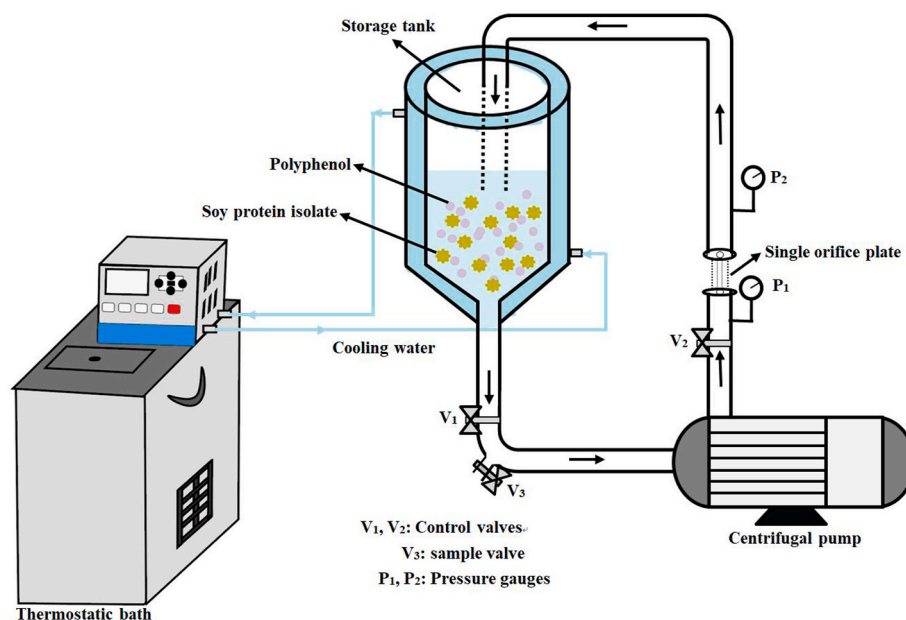


Fig. 1. Schematic diagram of the hydrodynamic cavitation (HC) device.

was turned on and the temperature was set at 10 °C to keep the temperature in the storage tank below 35 °C during operation, and then the device was started to treat the mixed solution for 30 min at a pressure of 1.5 bar. The above sample solutions were stored in a freezer at 4 °C for 12 h and then centrifuged at 8000 rpm for 20 min at 20 °C in a high-speed freeze centrifuge (Avanti JXN 26, Beckman Coulter Co., Ltd., CA, USA). The supernatant was dialyzed with a 3500 Da dialysis bag for 30 h, and the water was changed every 2–3 h to remove free polyphenols. Some samples were pre-frozen and vacuum lyophilized for 12 h and stored in sealed bags, and some samples were refrigerated directly in the freezer at 4 °C and set aside. The sample without HC treatment was magnetically stirred for 30 min instead of being subjected to HC treatment, and the other steps were conducted as described above.

2.3. Determination of binding polyphenol amounts

The Folin–Ciocalteu method was used to evaluate polyphenol binding levels as previously described, with slight modifications (Ballon et al., 2024). Briefly, the sample solutions were diluted with deionized water to achieve a protein concentration of 1 mg/mL. Subsequently, 1 mL of each diluted solution was mixed with 0.5 mL of Folin–Ciocalteu reagent (0.2 M) and incubated for 5 min in the dark. Next, 3 mL of sodium carbonate solution (6%, w/v) was added, and the mixture was allowed to react for 1 h in the dark at 25 °C. Finally, the absorbance was recorded at 760 nm using an ultraviolet–visible spectrophotometer (UV 5100H, Metash Instrument Co., Ltd., Shanghai, China), and deionized water was used instead of sample solution in the control. Standard curves were drawn using TA, CGA, FA, CA, and GA as standards, and each standard curve of polyphenol was used to determine the polyphenol binding level (TA: $y = 23.922x + 0.0237$, $R^2 = 0.9998$; CGA: $y = 16.542x + 0.0175$, $R^2 = 0.9998$; FA: $y = 19.146x + 0.0446$, $R^2 = 0.9998$; CA: $y = 28.099x - 0.0123$, $R^2 = 0.9999$; GA: $y = 26.482x + 0.0314$, $R^2 = 0.9992$). Polyphenol binding was expressed as follows:

$$\text{Polyphenol binding (\%)} = \frac{\text{Polyphenol in sample (mg)}}{\text{Total polyphenol (mg)}} \times 100\% \quad (1)$$

2.4. Measurement of free sulfhydryl groups

Tris-glycine buffer (pH 8) was prepared as described by Kang et al. (2016); briefly, 2.6 g of Tris, 1.69 g of glycine, 0.3725 g of EDTA-2Na, and 120.12 g of urea were dissolved in deionized water and then diluted to a final volume of 100 mL. The Ellman reagent was prepared by dissolving 40 mg of DTNB in 10 mL of Tris-glycine buffer. One milliliter of sample solution (10 mg/mL) was added to 4 mL of Tris-glycine buffer; subsequently, 50 μ L of Ellman reagent was added, and the mixture was incubated at 25 °C for 1 h. The absorbance at 412 nm was recorded as A_1 . Deionized water was used to replace the sample as a blank reagent. Tris-glycine buffer (50 μ L) was used instead of Ellman reagent (50 μ L) for the control group, and the absorbance was recorded as A_2 . The free sulfhydryl content of the sample was expressed as follows:

$$-\text{SH } (\mu\text{mol/g}) = (73.53 \times (A_1 - A_2) / C) \times D \quad (2)$$

Where D is the multiple of dilution of the sample, C is the concentration of protein, 73.53 is the molar absorptivity ($10^6/(1.36 \times 10^4)$), and 1.36×10^4 is the molar extinction coefficient.

2.5. Measurement of free amino groups

The quantity of free amino groups was determined by the OPA method described by Yan et al. (2021), with slight modifications. The OPA reagent was prepared as follows: 0.2 g of OPA was dissolved in 5 mL of methanol and then mixed with 12.5 mL of sodium dodecyl sulfate (SDS) solution (20 mg/mL), 125 mL of borax solution (0.1 M) and 0.5

mL of β -mercaptoethanol. Then, deionized water was added to the mixture until the total volume reached 250 mL. Subsequently, 200 μ L of the sample solution (5 mg/mL) was added to 4 mL of the OPA reagent and reacted in a 35 °C water bath for 5 min. The absorbance of the sample was determined at 340 nm. The sample was replaced with deionized water in the control. According to the above method, the absorption value-concentration of the L-leucine standard curve was drawn. Then, the free amino group content was calculated according to the standard curve.

2.6. Measurement of ultraviolet–visible spectroscopy

Each sample was diluted to 0.4 mg/mL (protein concentration) with deionized water. The sample solution was scanned at medium speed by an ultraviolet spectrophotometer (UV 2600, Shimadzu Instrument Co., Ltd., Suzhou, China) in the range of 200–400 nm to obtain the ultraviolet–visible spectrum. Deionized water was used as the reference solution.

2.7. Measurement of endogenous fluorescence spectroscopy

The fluorescence spectra were determined as previously described Liu et al. (2023a), with slight modifications. Briefly, each sample solution was diluted to 0.4 mg/mL with deionized water, and the sample solution was measured using a fluorescence spectrometer (G9800A, Agilent Technologies Co., Ltd., CA, USA). The excitation wavelength was 280 nm, the emission wavelength was in the range of 300–400 nm, and the excitation and emission slit wavelengths were both 5 nm.

2.8. Measurement of surface hydrophobicity (H_0)

H_0 was determined by using 1,8-ANS as a fluorescence probe, as described by Pan et al. (2023). The sample solutions were diluted to 0.25, 0.50, 0.75, 1.00, and 1.25 mg/mL with deionized water. Four milliliters of each diluent was mixed with 20 μ L of ANS solution (8 mM, dissolved in anhydrous ethanol) and then reacted for 20 min in the dark. The fluorescence intensity of the sample was determined using a fluorescence spectrometer. The excitation wavelength was 390 nm, the emission wavelength was 470 nm, and the slit width was 5 nm. The linear regression line was obtained by protein concentration and fluorescence intensity, and the slope of the linear regression equation was used as the H_0 of the sample.

2.9. Fourier transform infrared spectroscopy

Each freeze-dried sample powder was mixed with potassium bromide at a ratio of 1:100, pressed into a thin sheet, and analyzed using an Fourier transform infrared spectrometer (Cary-660, Shanghai Linli Instrument Co., Ltd., Shanghai, China) (Liao et al., 2024). Potassium bromide was used as the blank control. The spectroscopy scanning range was 400 to 4000 cm^{-1} , the resolution was 4 cm^{-1} , and the scanning frequency was 32 times/s. The data were processed using Peak Fit 4.12 software for baseline correction, smoothing, and curve fitting.

2.10. Circular dichroism spectroscopy

Each sample was diluted to 0.050 mg/mL with deionized water. Then, the sample was scanned by a far-UV instrument (Chirascan V100, Applied Photophysics Ltd., Surrey, UK) with continuous nitrogen filling, a scanning range of 190–250 nm, a rate of 100 nm/min, a spectral interval of 0.1 nm, an experimental temperature of 25 °C, and a sensitivity of 100 mdeg/cm. The percentages of α -helix, β -turns, β -sheets, and random coils in the protein were calculated using CDNN software.

2.11. Antioxidant properties

The DPPH· radical scavenging rate, ABTS⁺ radical scavenging rate, and ferric ion reducing antioxidant power (FRAP) of each sample were determined using an ultraviolet–visible spectrophotometer, as described by Gu et al. (2017) and Parolia et al. (2022).

2.11.1. DPPH· radical scavenging rate

Three milliliters of each sample solution (0.18 mg/mL) and 3 mL of DPPH·-ethanol solution (0.1 mM) were mixed and reacted for 1 h in the dark at room temperature. The absorbance was recorded at 517 nm. The DPPH· radical scavenging rate was calculated as follows:

$$\text{DPPH· radical scavenging rate (\%)} = (1 - (A_1 - A_2) / A_0) \times 100 \% \quad (3)$$

Where A_0 , A_1 , and A_2 represent the absorbance of deionized water reacting with DPPH·-ethanol solution, sample solution reacting with DPPH·-ethanol solution, and sample solution reacting with deionized water, respectively.

2.11.2. ABTS⁺ radical scavenging rate

The ABTS⁺ stock solution was prepared by mixing 7 mM ABTS⁺ solution (dissolved in 0.2 M PBS, pH 7.4) with 2.5 mM potassium persulfate solution (dissolved in 0.2 M PBS, pH 7.4) at a volume ratio of 1:1 and then reacting for 12–16 h at 25 °C. Before use, the stock solution was diluted with PBS (0.2 M, pH 7.4) until the absorbance at 734 nm reached 0.70 ± 0.02 . Subsequently, 2 mL of each sample solution (0.1 mg/mL) was mixed with 4.5 mL of the diluted ABTS⁺ solution. The mixture was allowed to react for 30 min in the dark at 25 °C, and the absorbance was determined at 734 nm. The ABTS⁺ radical scavenging rate was expressed as follows:

$$\text{ABTS}^+ \text{ radical scavenging rate (\%)} = (1 - (A_1 - A_2) / A_0) \times 100 \% \quad (4)$$

Where A_0 , A_1 , and A_2 represent the absorbance of deionized water reacting with diluted ABTS⁺ solution, the sample solution reacting with diluted ABTS⁺ solution, and the sample solution reacting with deionized water, respectively.

2.11.3. FRAP

A total of 0.3 mL of sample solution (10 mg/mL) was mixed with 3.0 mL of PBS (0.2 M, pH 6.6) and 3.0 mL of potassium ferricyanide solution (1%, w/v) and then reacted in a water bath at 50 °C for 30 min. The mixture was cooled to 25 °C, 3.0 mL of trichloroacetic acid solution (10%, w/v) was added, and the mixture was reacted for 20 min. The above solution was centrifuged at 5000 rpm for 10 min, and then 2.0 mL of supernatant was diluted with 4.0 mL of deionized water, mixed with 0.5 mL of ferric chloride solution (0.1%, w/v), and then reacted for 10 min at 25 °C. The absorbance was determined at 700 nm, and the absorbance value indicated the ferric ion reduction ability of the solution. Deionized water replaced the sample in the blank control.

2.12. Measurement of emulsification properties

The emulsification properties of the sample were expressed by the emulsifying activity index (EAI) and emulsifying stability index (ESI), as described by Yan et al. (2021). Briefly, 20 mL of each sample solution (10 mg/mL) was mixed with 5 mL of soybean oil and then homogenized at 10,000 rpm for 2 min by a high-speed homogenizer (Ultraturrax T25, IKA, Königswinter, Germany) to form an emulsion. Next, at 0 and 10 min, respectively, 20 µL of emulsion was absorbed from the bottom of the beaker and then added to 8 mL of SDS solution (0.1%, w/v). SDS solution was used in the blank control. The absorbance value was measured at 500 nm using an ultraviolet–visible spectrophotometer. The EAI and ESI of the sample solution were expressed as follows:

$$\text{EAI (m}^2/\text{g)} = (2.303 \times 2 \times A_0 \times F) / (10000 \times \theta \times C) \times 1000 \quad (5)$$

$$\text{ESI (min)} = A_0 / (A_0 - A_{10}) \times 10 \quad (6)$$

Where A_0 and A_{10} represent the absorbance measured at 0 and 10 min, respectively. F , θ , and C represent the sample dilution factor, the volume fraction of soybean oil, and the concentration of protein (mg/mL), respectively.

2.13. Statistical analysis

The experimental data were obtained from at least three repeated experiments, all of which were expressed as the mean \pm standard deviation (SD). IBM SPSS Statistics software (version 21.0, IBM Corp. Almonk, NY, USA) was used to analyze the differences. The Duncan test of one-way variance was used to analyze significant differences ($P < 0.05$ indicated a significant difference). Origin software (version 2017, OriginLab Corp. Northampton, MA, USA) was used to construct the graphs.

3. Results and discussion

3.1. Analysis of polyphenol binding

As shown in Fig. 2A, the quantity of polyphenols bound without HC treatment was ranked in the following order: TA > CGA > FA > CA > GA. The significant differences in binding amount among various polyphenols were related to differences in the molecular weight, number, and position of the hydroxyl groups of the polyphenols (Wang et al., 2024). As shown in Table 1, these five polyphenols exhibited substantial differences in molecular weight and structure. Among these polyphenols, TA demonstrated the highest binding degree, which could be attributed to its significantly greater molecular weight and number of phenolic hydroxyl groups compared to those of other polyphenols (Meng and Li, 2021). Similarly, Meng and Li (2021) compared the binding ability of three polyphenols (GA, CA, and EGCG) with that of whey protein isolate, suggesting that EGCG, which had a high phenolic hydroxyl number and molecular weight, had a high binding equivalent. The results indicated that polyphenols with higher molecular weights and more phenolic hydroxyl groups were more prone to binding.

As shown in Fig. 2A, the binding degree of polyphenols significantly increased after HC treatment compared to that of samples without HC treatment ($P < 0.05$), which might be ascribed to the mechanical and chemical effects of HC treatment: 1) The cavitation effects, such as high-speed shear and microjets generated by HC, not only led to the unfolding of protein, expanding the spatial structure and exposing more binding sites, but also accelerated the collision between free polyphenols and protein (Geng et al., 2022), promoting the interaction between benzene rings and phenolic hydroxyl groups of polyphenols and protein side chain groups; 2) The hydroxyl radicals generated by HC treatment promoted the oxidation of polyphenols to quinones and covalent binding with protein side chain affinity groups (Zheng et al., 2023), or attacked the hydrogen atoms at the protein side chain to form intermediates, and then these intermediates were covalently bound to polyphenols (Liu et al., 2023b). However, the promoting effect of HC treatment on different polyphenols varied due to differences in molecular weight and structure. For instance, HC treatment increased the TA binding capacity by nearly 2 times and the CGA binding capacity by approximately 1.2 times. This might be because the molecular weight and the number of phenolic hydroxyl groups of CGA were much smaller than those of TA. However, after HC treatment, the binding capacities of FA, CA, and GA were 23.66 ± 2.04 , 23.26 ± 1.32 , and $24.11 \pm 1.21\%$, respectively. This indicated that the binding degrees of these three polyphenols to protein under HC treatment were similar. This similarity might be due to their similar molecular weights, similar numbers of phenolic hydroxyl groups, and analogous structural characteristics.

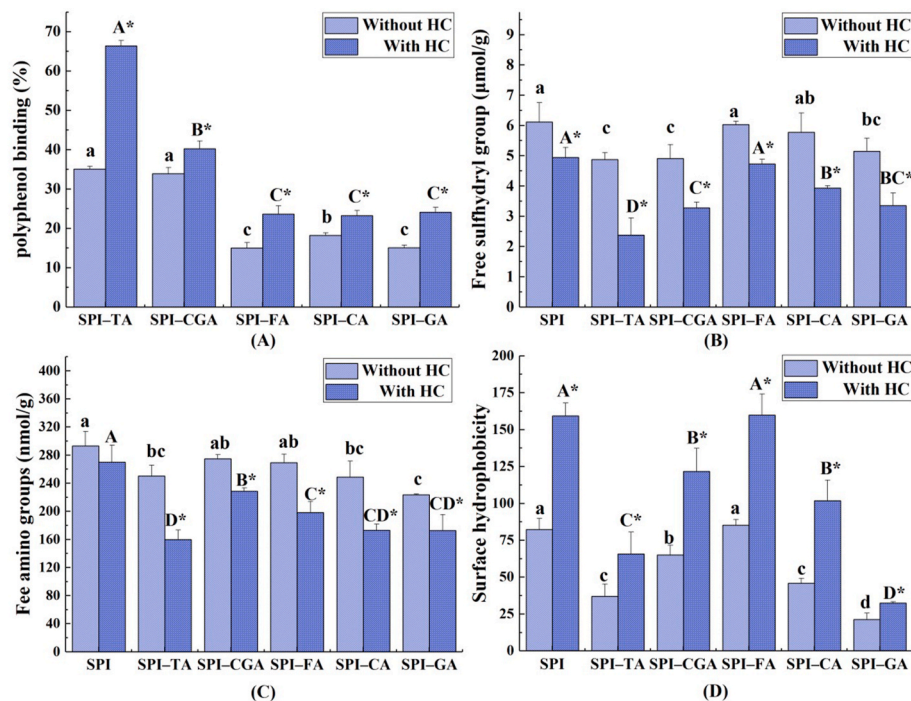


Fig. 2. Effects of HC treatment on polyphenol binding (A), free sulfhydryl groups (B), free amino groups (C), and surface hydrophobicity (D) of SPI and SPI-polyphenol complexes. Different lowercase and capital letters indicate significant differences in SPI and SPI-polyphenol complexes without and with HC treatment, respectively ($P < 0.05$). “*” indicates significant differences in SPI and SPI-polyphenol complexes without and with HC treatment ($P < 0.05$). SPI-TA: soy protein isolate-tannic acid complex; SPI-CGA: soy protein isolate-chlorogenic acid complex; SPI-FA: soy protein isolate-ferulic acid complex; SPI-CA: soy protein isolate-caffeic acid complex; SPI-GA: soy protein isolate-gallic acid complex.

3.2. Analysis of free sulfhydryl and amino groups

Polyphenols covalently bind to the free sulfhydryl and amino groups of protein through C-S and C-N bonds (Yan et al., 2021). During the determination of the free sulfhydryl groups in the protein, a urea solution was used to inhibit the conversion of sulfhydryl groups to disulfide bonds, while during the determination of the free amino groups in the protein, SDS solution was used to disrupt the noncovalent interactions (Yan et al., 2021). Therefore, the covalent interaction between protein and polyphenols can be evaluated by measuring the free sulfhydryl and amino groups.

As shown in Fig. 2B and C, without HC treatment, the quantities of free sulfhydryl and amino groups were slightly lower in the SPI-polyphenol complexes (except for the SPI-FA complex) than in SPI. This finding could be attributed to the fact that the polyphenols were inevitably oxidized to quinones when the samples were prepared under non-vacuum conditions, which subsequently formed C-S and C-N bonds with the free sulfhydryl and amino groups of SPI, resulting in a slight decrease in the amount of free sulfhydryl and amino groups (Li et al., 2021b). Furthermore, after HC treatment, the content of free amino groups in SPI had no significant change than that without HC treatment ($P > 0.05$), but the content of free sulfhydryl groups in SPI was significantly lower than that without HC treatment ($P < 0.05$). The decrease of the free sulfhydryl groups might be attributed to the oxidation and cross-linking of the protein sulfhydryl groups caused by the mechanical and chemical effects of HC treatment (Kang et al., 2016). The number of free sulfhydryl and amino groups in the SPI-polyphenol complexes after HC treatment was significantly lower than the number in the SPI-polyphenol complexes without HC treatment and the number in SPI with HC treatment alone ($P < 0.05$). This finding could be attributed to the fact that the hydroxyl radicals produced by HC treatment attacked the hydrogen atoms on free sulfhydryl and amino groups of protein to form protein free radicals, which reduced the number of sulfhydryl and amino groups by binding to the benzene ring of polyphenols via the C-S

and C-N bonds (Geng et al., 2022). These results were consistent with the research conducted by Mohammadi et al. (2023), which found that the hydroxyl radicals attacked the sulfhydryl and amino groups on the protein backbone to form protein radicals. These protein radicals then attacked the ortho and para positions of phenolic hydroxyl groups on polyphenols, forming protein-polyphenol conjugates through C-N and C-S bonds. This finding indicated that HC treatment promoted the covalent interaction between the polyphenols and the free sulfhydryl and amino groups of SPI, and further proved that the improvement of polyphenol binding ability after HC treatment was also related to the covalent interaction. Furthermore, there were significant differences in the contents of free sulfhydryl and amino groups among different SPI-polyphenol complexes, which might be related to the number and position of hydroxyl groups of polyphenols and the interaction between polyphenols and SPI. The model of the reaction between CGA and myofibrillar protein developed by Cao and Xiong (2015), which also showed that the free sulfhydryl and amino groups of the protein interacted with the ortho-position and para-position of phenolic hydroxyl groups of polyphenols through the C-S and C-N bonds.

3.3. Ultraviolet-visible spectroscopy analysis

The benzene rings of aromatic amino acids, such as tyrosine, tryptophan, and phenylalanine, contain conjugated double bonds; therefore, protein can absorb ultraviolet light. Additionally, the exposure of aromatic amino acid residues and changes in their microenvironment will lead to changes in protein absorption peak intensity and position (Chen and Ma, 2020). Hence, Ultraviolet-visible spectroscopy can be used to characterize the three-dimensional conformational changes in protein caused by interactions between protein and polyphenols.

As shown in Fig. 3A, without HC treatment, the absorption peak of SPI was at 273–274 nm, and the absorption intensity of the SPI-polyphenol complexes increased compared with that of SPI, indicating that the interaction between SPI and polyphenols formed a

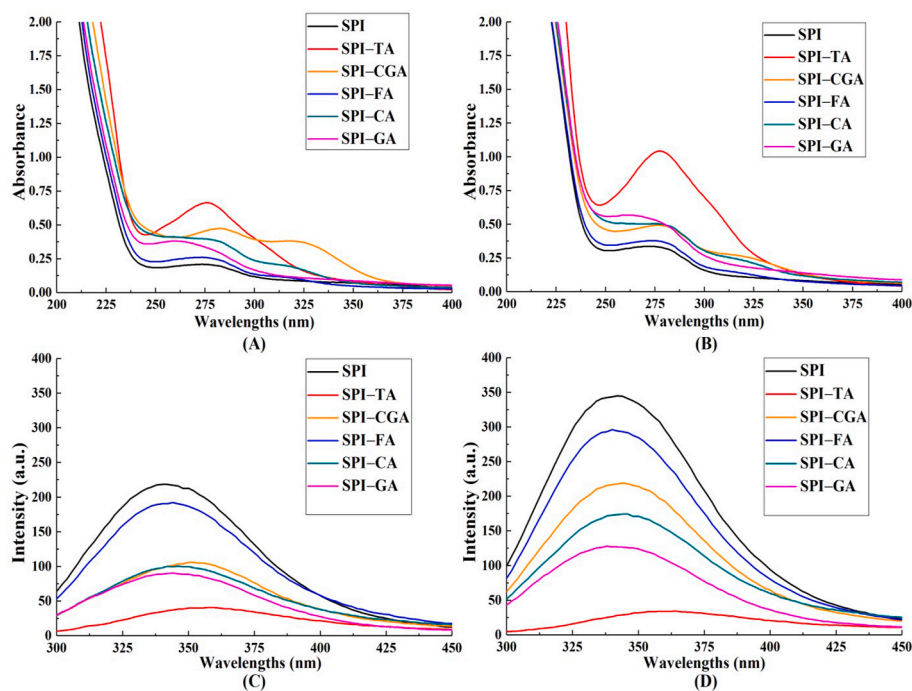


Fig. 3. Ultraviolet–visible spectroscopy (A without HC; B with HC) and endogenous fluorescence spectroscopy (C without HC; D with HC) of SPI and SPI–polyphenol complexes.

conjugated system, which reduced the energy required for the valence electrons to transition from π to π^* energy level, thus increasing the absorption intensity (Dai et al., 2024). Similar results were shown by Han et al. (2022), who reported that adding EGCG could enhance the absorption intensity of pea protein isolate. Notably, the absorption peak of the SPI–TA complex exhibited the greatest absorbance intensity and largest red shift, which might be attributable to TA's higher molecular weight, substantial number of benzene rings and phenolic hydroxyl groups, which increased the interaction between SPI and TA and introduced more benzene rings, resulting in a stronger conjugated system. Similarly, Dai et al. (2024) observed that the number of benzene rings in the system of the interaction of EGCG (with more molecular weight, benzene ring, and phenolic hydroxyl number) and SPI was more than that of catechins, forming a stronger conjugated system, resulting in a larger absorption intensity and redshift of the characteristic peak of SPI–EGCG complex. Moreover, the degree of TA binding to SPI was greater than that of the other polyphenols, as shown in section 3.1. The SPI–CGA and SPI–CA complexes exhibited new peaks at 310–340 nm, demonstrating that the interaction between polyphenols and SPI changed the structure of SPI. This result aligned with previous research showing that the interaction between perilla seed meal protein and apigenin generated a new peak between 350 and 400 nm in the Ultraviolet–visible spectroscopy, proving the change in the structure of the protein (Wang et al., 2024).

As shown in Fig. 3B, after HC treatment, the absorption peak of SPI remained at 273–274 nm; however, the absorbance intensity increased, indicating that HC treatment expanded the structure of SPI and exposed more aromatic amino acid residues (Zheng et al., 2023). After HC treatment, the absorption intensity of the SPI–polyphenol complexes increased compared with that of SPI (with HC treatment) and SPI–polyphenol complexes (without HC treatment), suggesting that HC treatment enhanced the interactions between SPI and polyphenols. This result was consistent with the increase of the binding level of polyphenols to SPI after HC treatment. Interestingly, compared with SPI, the absorption peaks of the SPI–TA, SPI–CGA and SPI–CA complexes were red-shifted to varying degrees by HC treatment. This could be attributed to two main factors: (1) the strength of the conjugated system formed by

SPI and TA, CGA, and CA; (2) the interaction of SPI with TA, CGA, and CA introduced different numbers of polar groups (such as hydroxyl and carboxyl groups), leading to the microenvironment with difference polarity when the valence electrons transitioned from π to π^* in the conjugated system. Additionally, the absorption peak of SPI–GA complex was blue-shift, which might be due to the interaction between the hydroxyl group of GA and the hydrophobic group of SPI, resulting in the exposure of hydrophobic group in SPI. Or, the covalent bonding between GA and SPI induced stretching of the SPI peptide chain, which exposed the hydrophobic groups originally hidden inside the tyrosine and tryptophan residues of SPI, and consequently changed the microenvironment around these residues (Chen et al., 2024a). The above results fully showed that the interaction between different polyphenols and SPI had different effects on the structure of SPI after HC treatment.

3.4. Endogenous fluorescence spectroscopy analysis

The alteration of the microenvironment polarity of tryptophan and tyrosine in protein changes the fluorescence intensity and maximum fluorescence emission wavelength (λ_{\max}) of the protein (Cao and Xiong, 2015). Therefore, the impact of polyphenols on the tertiary structure of protein can be revealed according to the fluorescence intensity and the shift in the λ_{\max} position.

As shown in Fig. 3C, without HC treatment, the fluorescence intensity of the SPI–polyphenol complexes was lower, and the λ_{\max} was red-shifted compared to that of the SPI. This finding might be attributable to the interaction between the aromatic rings and hydroxyl groups of polyphenols and the side chain groups of SPI, resulting in fluorescence quenching (Liao et al., 2024). Additionally, the interaction between polyphenols and SPI masked a portion of the hydrophobic region, introduced hydroxyl groups, and stretched the structure of SPI, thereby altering the polarity of the microenvironment of tryptophan and tyrosine residues (Sun et al., 2022). Notably, the decrease in the fluorescence intensity and red-shifting of the SPI–polyphenol complexes varied depending on the structure of the polyphenols and their interactions with the SPI. Among them, the SPI–TA complex exhibited the lowest fluorescence intensity and the most significant redshift, which could be

ascribed to the high molecular weight and the large number of hydroxyl groups in TA. Therefore, the interactions between TA and SPI introduced numerous additional hydroxyl groups, resulting in the tryptophan and tyrosine residues being located in more hydrophilic microenvironments.

As shown in Fig. 3D, after HC treatment, the fluorescence intensity of the SPI was significantly greater, and the λ_{\max} slightly red-shifted compared with that of untreated SPI. This finding might be ascribed to the HC treatment destroying the internal interactions of the SPI, stretching the SPI structure, exposing the internal tryptophan and tyrosine, and changing the polarity of the amino acid residues micro-environment. After HC treatment, the fluorescence intensity of the SPI-polyphenol complexes decreased compared with that of SPI, and the decrease was more obvious than that without HC treatment. This finding might be because HC treatment facilitated the involvement of more tryptophan and tyrosine residues in covalent interactions between polyphenols and SPI, thereby enhancing fluorescence quenching (Chen et al., 2024). These results were similar to those of Liu et al. (2023a), who discovered that ultrasonic treatment enhanced the interaction of β -lactoglobulin and CGA to form a complex, resulting in fluorescence quenching. However, after HC treatment, the change in the λ_{\max} of the SPI varied for the various polyphenols. TA, CGA, and CA demonstrated a red-shifted λ_{\max} , FA did not change the λ_{\max} , and GA demonstrated a slightly blue-shifted λ_{\max} . This finding might be due to the interaction between TA, CGA, and CA and SPI, resulting in more exposure of the tryptophan and tyrosine residues to the polar environment under these conditions. The interactions between GA and SPI resulted in the reburying of tryptophan and tyrosine residues in SPI or the release of more hydrophobic amino acids, causing tryptophan and tyrosine residues to reside in a relatively hydrophobic environment. This result indicated that HC treatment had different effects on the interaction between SPI and diverse polyphenols.

3.5. H_0 analysis

H_0 reflects the exposure of the hydrophobic groups on the protein surface and the change in protein conformation, which is closely related to emulsification and solubility. ANS is typically used as a fluorescence probe for determining the H_0 value (Liao et al., 2024). As shown in Fig. 2D, without HC treatment, the H_0 of the SPI-polyphenol complexes significantly decreased (except for that of the SPI-FA complex) compared with that of the SPI ($P < 0.05$). This decrease was ascribed to the hydrophobic interaction between the nonpolar aromatic ring of polyphenols and the hydrophobic amino acid residues of SPI (Sun et al., 2022), which shielded some of the hydrophobic region of SPI, reducing the binding of ANS to the hydrophobic region and subsequently decreasing the H_0 value. Additionally, interactions between the benzene ring of polyphenols and the sulfhydryl and amino groups of protein introduced polar groups, such as hydroxyl and carboxyl groups, which decreased H_0 (Meng and Li, 2021). Liu et al. (2024) reported the similar results that EGCG, CGA, and piceatannol enhanced the hydrophilicity of wheat germ protein by introducing hydroxyl groups during their interacting with wheat germ protein, thereby reducing the H_0 . However, the addition of FA did not cause a significant change in the H_0 of SPI ($P > 0.05$), which might be due to the low number hydroxyl groups of FA and low binding to SPI.

As shown in Fig. 2D, after HC treatment, the H_0 of SPI increased significantly by approximately 2 times ($P < 0.05$). This finding was attributed to the destruction of the SPI interaction by high-speed shear force, hydroxyl radicals, and heat generated by HC treatment (Liu et al., 2023), resulting in stretching of the structure and conformational rearrangement that exposed internal hydrophobic groups. After HC treatment, the H_0 of the SPI-polyphenol complexes (except for the SPI-FA complex) was significantly lower than that of SPI ($P < 0.05$), and the degree of decrease was greater than that without HC treatment. This result could be attributable to the HC treatment promoting the exposure of hydrophobic groups on the surface of the SPI, thus increasing the

number of binding sites for polyphenols and SPI interactions; under the action of free radicals and the mechanical effects of HC, the enhanced interactions between SPI and TA, CGA, CA, and GA led to the introduction of a large number of hydroxyl and carboxyl groups, decreasing the H_0 .

3.6. Fourier transform infrared spectroscopy analysis

Fourier transform infrared spectroscopy characterizes the interactions between protein and polyphenols and the changes in protein structure according to the shift in the absorption peak position. Fig. 4A and B showed that adding polyphenols and HC treatment shifted the wavenumber corresponding to the typical absorption peak of SPI (or SPI-polyphenol complexes), indicating a change in the structure of the SPI.

As shown in Fig. 4A, without HC treatment, the typical peaks of the SPI were at 3291.3 cm^{-1} (N-H stretching and O-H stretching), 2960.6 cm^{-1} ($-\text{CH}_2$ asymmetric stretching vibration), 1658.9 cm^{-1} (C=O stretching vibration), 1537.5 cm^{-1} (C-N stretching vibration and N-H bending vibration), and 1238.5 cm^{-1} (N-H bending vibration and C-N stretching vibration), which were located in the amide A, B, I, II, and III bands, respectively (Jeong et al., 2013; Li et al., 2023). Additionally, the peak at 1081.1 cm^{-1} represented the stretching vibration of the C-O bond (Dai et al., 2024). Without HC treatment, the typical peaks in the amide A band of the SPI-TA, SPI-FA, and SPI-GA complexes exhibited different degrees of red-shifting compared with those of SPI, which was attributed to interactions between the hydroxyl and carboxyl groups of the polyphenols and the N-H groups on the SPI that formed hydrogen bonds (Jeong et al., 2013). Moreover, CGA and CA resulted in blue-shifting of the typical peak in the amide A band to varying extents, demonstrating that introducing phenolic hydroxyl groups enhances O-H bond stretching vibrations within interactions between polyphenols and SPI (Li et al., 2023). Furthermore, the typical peak in the amide I/II band of the SPI-polyphenol complexes also showed red- and blue-shifting. The red-shift indicated that more hydrogen bonds existed within the SPI-polyphenol complexes, and electrostatic interactions existed between the polyphenols and the SPI (Dai et al., 2018). Conversely, the blue-shift indicated that the benzene ring and carbon chain of the polyphenols interacted with the hydrophobic amino acid residues of SPI. These results aligned with those of Liao et al. (2024), who reported that TA, EGCG, and GA caused a blue-shift of the typical peaks in the amide I/II bands of protein, which might be related to hydrophobic interactions between them. The above results indicated that the change in the structure of SPI through hydrogen bonding, electrostatic interactions, and hydrophobic interactions between polyphenols and SPI. The different changes in the typical peaks in the amide A, I and II bands might be related to the different types and structures of polyphenols.

As shown in Fig. 4B, after HC treatment, the typical peak in the amide A band of SPI was blue-shifted, while that of the amide II band was red-shifted, demonstrating that HC treatment changed the stretching vibration of the O-H and C-N groups and the bending vibration of the N-H groups of SPI. This finding was attributed to the fact that the bursting of cavitation bubbles generated by HC treatment was accompanied by high-speed shear force, instantaneous high temperature, and hydroxyl radicals, inducing SPI unfolding and aggregation, which changed the secondary structure of the SPI. After HC treatment, compared with that of SPI, the red-shift of the typical peak in the amide A band of SPI-polyphenol complexes was attributed to the presence of more binding sites on the SPI due to HC treatment, which promoted the formation of hydrogen bonds between the SPI and the polyphenols. In addition, the hydroxyl radical generated by HC treatment induced the oxidation of polyphenols to quinones, which then formed C-N bonds with nucleophilic groups on SPI, resulting in peak shifts (Fei et al., 2023). Furthermore, after HC treatment, the typical peak in the amide I and II bands of the SPI-polyphenol complexes also blue- and red-shifted to varying degrees compared with those of SPI. This result was slightly

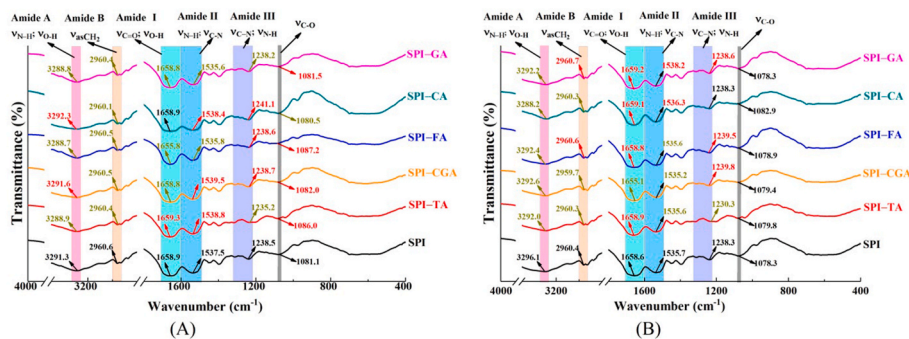


Fig. 4. (A) Fourier transform infrared spectroscopy of SPI and SPI-polyphenol complexes without HC, (B) Fourier transform infrared spectroscopy of SPI and SPI-polyphenol complexes with HC.

different from that without HC treatment, indicating that HC treatment altered the interactions between polyphenols and SPI. After HC treatment, the typical peak in the amide A band of the SPI-polyphenol complexes showed a blue-shift (except for the SPI-CA complex), the typical peak in the amide I band exhibited a red-shift (SPI-TA and SPI-CGA complexes) and a blue-shift (SPI-FA, SPI-CA, and SPI-GA complexes), and the typical peak in the amide II band exhibited a red-shift. The blue-shift of the typical peak in the amide A band was ascribed to interactions between polyphenols and SPI, which introduced more hydroxyl groups and enhanced the O-H bond stretching vibration. The red-shift of the typical peak in the amide I/II band was attributed to interactions between SPI and polyphenols to form C-N bonds (Yan et al., 2021), demonstrating that covalent interactions existed between the polyphenols and SPI. Additionally, the blue-shift of the typical peak in the amide I band was caused by the extension of SPI structure after HC treatment, which promoted the hydrophobic interactions of FA, CA, and GA with SPI.

3.7. Circular dichroism spectroscopy analysis

Circular dichroism spectroscopy is used to characterize changes in the secondary structure of a protein. As shown in Fig. 5A and B, SPI exhibited a negative peak corresponding to the α -helix near 210 nm and a positive peak corresponding to the β -sheet near 190 nm. The specific α -helix, β -sheet, β -turn, and random coil content data for the SPI and SPI-polyphenol complexes were presented in Table 2. Without HC treatment, adding polyphenols significantly increased the α -helix, β -turn, and random coil contents and decreased the β -sheet content within the SPI structure ($P < 0.05$). The decrease in the β -sheet content and increase in the β -turn content and random coil content were ascribed to interactions between the polyphenols and SPI, which

resulted in the local breaking of regular hydrogen bonds, the looseness of peptide chains, and the extension of the SPI structure (Zhou et al., 2020). The increase in the α -helix content was linked to interactions between the phenolic hydroxyl groups of polyphenols and the carbonyl and amino groups of SPI, which increased intramolecular hydrogen bonding within the polypeptide chain and rearrangement, promoting local peptide chain disorder (Wang et al., 2021b). Similar findings were reported by Li et al. (2020a), in which the combination of different phenolic acids with β -lactoglobulin caused secondary structure transition from β -sheet to β -turn and α -helix, leading to partial instability of the β -lactoglobulin conformation. However, Pi et al. (2023) focused on the preparation of covalent SPI-anthocyanin complexes under alkaline conditions and found that the addition of anthocyanins reduced the content of α -helix and β -turn in SPI, while increasing the content of β -sheet and random coil. These differences might be attributed to variations in the types of polyphenols, protein types, and treatment methods, which resulted in changes in the interaction mode and binding sites between polyphenols and protein, ultimately leading to different alterations in the secondary structure of protein.

After HC treatment, the contents of α -helix, β -turn, and random coil in the SPI increased significantly, whereas the content of β -sheet decreased significantly ($P < 0.05$). This finding was attributed to the fact that the high-speed shear force generated by HC treatment broke the intermolecular hydrogen bonds that maintain the stability of the β -sheet structure, loosening the peptide chain. Moreover, under the action of the cavitation effect produced by the bursting of the cavitation bubble, hydrogen bonds were reconstructed between the carbonyl groups and the amino groups in the local peptide chain, increasing the content of the α -helix (Xie et al., 2024). However, after HC treatment, compared with those of the SPI, the contents of α -helix (except for the SPI-CGA complex) and random coil of the SPI-polyphenol complexes increased

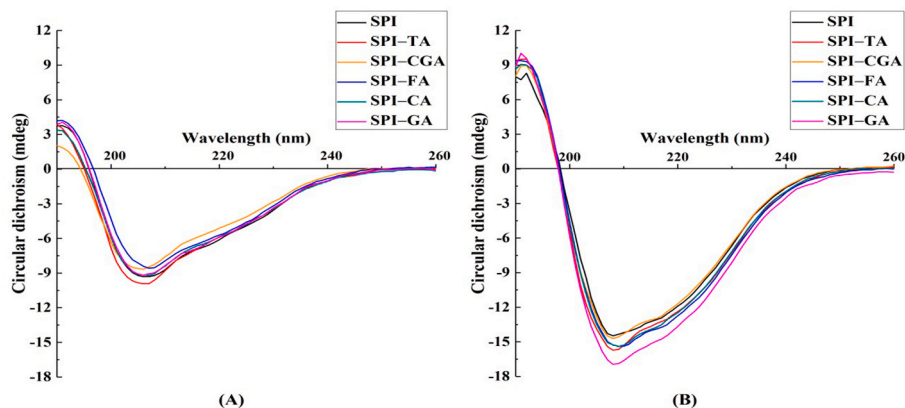


Fig. 5. (A) Circular dichroism spectroscopy of SPI and SPI-polyphenol complexes without HC, (B) Circular dichroism spectroscopy of SPI and SPI-polyphenol complexes with HC.

Table 2

The secondary structure of the SPI and SPI–polyphenol complexes with or without HC treatment.

Treatment methods	Sample	Content (%)			
		α -helix	β -sheet	β -turn	Random coil
Without HC	SPI	15.88 \pm 0.58 ^d	43.19 \pm 0.72 ^a	16.91 \pm 0.12 ^c	23.99 \pm 0.17 ^c
	SPI–TA	20.32 \pm 0.01 ^a	36.42 \pm 0.18 ^c	17.70 \pm 0.01 ^a	25.52 \pm 0.27 ^b
	SPI–CGA	18.64 \pm 0.37 ^c	38.23 \pm 0.06 ^b	17.40 \pm 0.11 ^b	25.73 \pm 0.62 ^b
	SPI–FA	20.44 \pm 0.08 ^a	34.83 \pm 0.54 ^d	17.55 \pm 0.04 ^b	27.18 \pm 0.53 ^a
	SPI–CA	19.39 \pm 0.61 ^b	36.02 \pm 0.27 ^c	17.44 \pm 0.16 ^b	27.23 \pm 0.51 ^a
	SPI–GA	20.57 \pm 0.22 ^a	34.96 \pm 0.19 ^d	17.59 \pm 0.06 ^{ab}	26.86 \pm 0.23 ^a
With HC	SPI	20.51 \pm 0.29 ^{C*}	33.85 \pm 0.43 ^{A*}	17.44 \pm 0.04 ^{AB*}	28.23 \pm 0.01 ^{B*}
	SPI–TA	21.16 \pm 0.00 ^{B*}	32.06 \pm 0.10 ^{BC*}	17.42 \pm 0.00 ^{AB*}	29.45 \pm 0.10 ^{A*}
	SPI–CGA	20.52 \pm 0.52 ^{C*}	32.60 \pm 0.57 ^{B*}	17.27 \pm 0.11 ^C	29.55 \pm 0.23 ^{A*}
	SPI–FA	21.15 \pm 0.36 ^{B*}	31.76 \pm 0.35 ^{C*}	17.33 \pm 0.02 ^{BC*}	29.80 \pm 0.10 ^{A*}
	SPI–CA	20.82 \pm 0.30 ^{BC*}	32.01 \pm 0.26 ^{BC*}	17.28 \pm 0.12 ^C	29.92 \pm 0.54 ^{A*}
	SPI–GA	21.99 \pm 0.13 ^{A*}	31.09 \pm 0.30 ^{D*}	17.51 \pm 0.03 ^A	29.44 \pm 0.37 ^{A*}

Different lowercase and capital letters indicate significant differences in SPI and SPI–polyphenol complexes without and with HC treatment, respectively ($P < 0.05$). “*” indicates significant differences in SPI–polyphenol complexes without and with HC treatment.

significantly, whereas the contents of β -sheet and β -turn (except for the SPI–TA and SPI–GA complexes) decreased significantly ($P < 0.05$). This finding might be ascribed to the cavitation effect of HC treatment, which unfolded SPI and exposed more hydrophobic regions and free amino groups, promoting the hydrophobic interaction between polyphenols and SPI and the formation of hydrogen bonds, leading to a change in the secondary structure of SPI (Zhang et al., 2020). Apparently, for the same polyphenol, compared with those without HC treatment, the α -helix and random coil contents in SPI–polyphenol complexes significantly increased ($P < 0.05$). This might be due to the cavitation effect facilitating the stretching of the SPI structure, which was conducive to the interaction of exposed hydrophobic amino acid residues with hydroxyl groups, carboxyl groups, and benzene rings of polyphenols, resulting in the rearrangement of polypeptide chains. On the other hand, the β -sheet content significantly decreased ($P < 0.05$), which might be attributed to

the destruction of regular hydrogen bonds in the SPI structure by HC treatment, resulting in partial disintegration or loosening of the SPI structure.

3.8. Analysis of antioxidant properties

The antioxidant activities of the SPI and SPI–polyphenol complexes with or without HC treatment were evaluated by determining the DPPH· and ABTS⁺ radical scavenging rates and the FRAP. The hydroxyl groups on the aromatic ring of polyphenols can provide electrons or H⁺ to neutralize free radicals and play a role in scavenging free radicals (Tian et al., 2021). As shown in Fig. 6A, B, and C, without HC treatment, the DPPH· and ABTS⁺ radical scavenging rates and FRAP of SPI–polyphenol complexes were significantly greater than those of SPI ($P < 0.05$). This finding was attributed to the interactions between polyphenols and SPI,

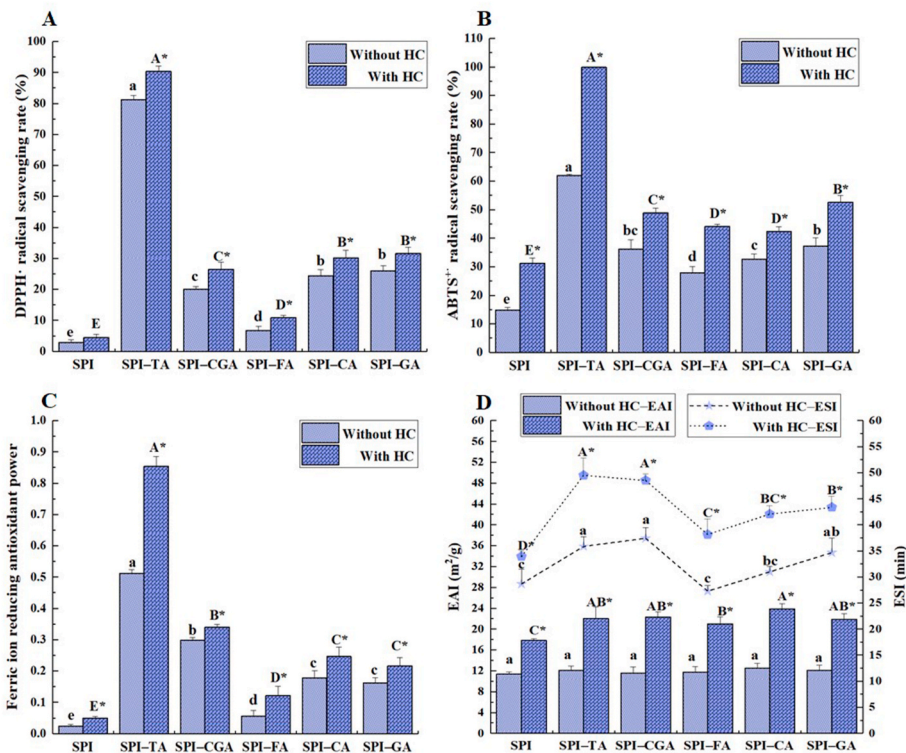


Fig. 6. Effects of HC treatment on the DPPH· radical scavenging rate (A), ABTS⁺ radical scavenging rate (B), ferric ion reducing antioxidant power (C), emulsifying activity (EAI) (D), and emulsifying stability (ESI) (D) of SPI and SPI–polyphenol complexes. Different lowercase and capital letters indicate significant differences in SPI and SPI–polyphenol complexes without and with HC treatment ($P < 0.05$). “*” indicates significant differences in SPI–polyphenol complexes without and with HC treatment.

which introduced a large number of hydroxyl and carboxyl groups. These two groups not only gave SPI antioxidant properties as proton donors, but also provided electrons for Fe^{3+} , imparting a reduction ability to SPI (Parolia et al., 2022). Similar results were discovered in previous studies by Geng et al. (2022), where the combination of SPI and EGCG introduced a large number of hydroxyl groups, significantly enhancing the antioxidant activities of the SPI. Additionally, the DPPH· and ABTS⁺ radical scavenging rates and FRAP of the SPI-TA complex were the highest, which might be related to the large number of hydroxyl groups introduced by the interaction between SPI and TA, and the strongest binding ability of TA to SPI among the five polyphenols (as shown in section 3.1). Although the higher binding degree of CGA to SPI compared to GA, the free radical scavenging ability of the SPI-GA complex was greater than that of the SPI-CGA complex, which might be related to the structures of GA and CGA. GA contains 3 phenolic hydroxyl groups, CGA contains 2 phenolic hydroxyl groups and 3 hydroxyl groups, and the activity of the hydroxyl groups is less than that of the phenolic hydroxyl groups; therefore, the antioxidant activity of the SPI-CGA complex was slightly lower than that of the SPI-GA complex. Chen et al. (2024a) also showed that the number and location of polyphenol hydroxyl groups affected the antioxidant capacity of quinoa protein isolate-polyphenol conjugates. Overall, there were differences in the antioxidant activity among the SPI-polyphenol complexes, which might be due to variations in the molecular weight, hydroxyl number, and position of the polyphenols, as well as differences in the interaction mechanism and binding amount between the polyphenols and SPI.

After HC treatment, the DPPH· and ABTS⁺ radical scavenging rates, and FRAP of the SPI were significantly enhanced ($P < 0.05$), demonstrating that the shear effect produced by HC treatment stretched the structure of the SPI and exposed more amino acid residues (such as tryptophan, phenylalanine, and methionine). These amino acid residues could be used as hydrogen donors to improve the antioxidant capacity of SPI (Wen et al., 2022). Similarly, Bhimrao Muley et al. (2020) also found that the hydrophobic and aromatic amino acids in whey protein isolate hydrolysates could be used as proton donors, thus enhancing the free radical scavenging ability of whey protein isolate hydrolysates. After HC treatment, the DPPH· and ABTS⁺ radical scavenging rates and FRAP of the SPI-polyphenol complexes were also significantly greater than those of the SPI (with HC treatment) and the SPI-polyphenol complexes (without HC treatment) ($P < 0.05$). This result was ascribed to the fact that HC treatment facilitated the binding of more polyphenols to SPI and introduced functional groups such as phenolic hydroxyl groups and carboxyl groups, thereby enhancing the antioxidant capacity of SPI (Gu et al., 2017). Similarly, Chen et al. (2022) found ultrasonic treatment facilitated the interaction between SPI and EGCG, thereby enhancing the antioxidant activity.

3.9. Emulsification analysis

EAI refers to the ability of protein to rapidly disperse at the oil-water interface and reduce their interfacial tension to form emulsions, while ESI refers to the ability of an emulsion to resist flocculation or delamination and maintain dispersion after droplet formation (Li et al., 2020b). The changes in the EAI and ESI of SPI and the SPI-polyphenol complexes with and without HC treatment were shown in Fig. 6D.

Without HC treatment, the addition of five polyphenols had no significant effect on the EAI of SPI ($P > 0.05$), which meant that the existence of the polyphenols did not hinder the ability of the SPI to form emulsions. This result was consistent with previous findings showing that the addition of EGCG did not affect the EAI of lactoferrin (Li et al., 2021). However, the ESI of the SPI-polyphenol complexes (except for the SPI-FA complex) increased significantly ($P < 0.05$), possibly due to the interactions between the polyphenols and SPI altering the surface groups and increasing the flexibility of the SPI. Additionally, as shown in 2D, the addition of polyphenols reduced the H_0 of SPI, which reduced the hydrophobic attraction between droplets, thus enhancing its ability

to resist droplet aggregation (Li et al., 2021a). There were also differences in the ESI among the SPI-polyphenol complexes, which might be attributable to the different interaction modes between diverse polyphenols and SPI, resulting in different effects on the structure. For example, the ESI of the SPI-TA complex was significantly greater than that of the SPI-FA complex ($P < 0.05$), which could be attributed to the strong binding ability of TA to SPI, which greatly influenced the hydrophilic/lipophilic balance of SPI. These findings aligned with those of Pan et al. (2023), who reported that different polyphenols produced distinct modifications to the structure of bovine bone protein, resulting in different effects on the EAI and ESI.

After HC treatment, the EAI and ESI of SPI significantly increased ($P < 0.05$), which was ascribed to the fact that HC treatment promoted SPI unfolding, altered its conformation, and enhanced its absorption in the oil-water interface (Wang et al., 2021a). After HC treatment, the EAI and ESI of the SPI-polyphenol complexes were significantly greater ($P < 0.05$) than those of SPI (with HC treatment) and SPI-polyphenol complexes (without HC treatment). This was attributed to the shearing effect and free radical effect of HC treatment, which promoted the binding of polyphenols to SPI, thereby increasing their electrostatic repulsion and spatial hindrance. Consequently, this reduced the accumulation of oil droplets and increased the steric hindrance between droplets. Zhang et al. (2025) also reported that EGCG conjugated with legume protein increased the inter-particle spacing and electrostatic repulsion, reducing oil droplet aggregation and enhancing emulsification. And higher EGCG grafting rates further improved emulsification performance. Moreover, the free radical effect facilitated covalent interactions between the polyphenols and SPI, altering the exposure of the hydrophobic and hydrophilic groups on the SPI surface and thereby improving the SPI hydrophilic/lipophilic balance. After HC treatment, the increase in the random coil contents in the SPI-polyphenol complexes could increase their flexibility, thereby improving their ability to adsorb at the oil-water interface. Similarly, Pi et al. (2023) demonstrated that the improvement in the emulsification properties of SPI was associated with an increase in random coil content when proanthocyanidins was combined with SPI. These findings confirmed that the SPI-polyphenol complexes treated with HC exhibited higher emulsifying properties.

4. Conclusion

In this study, the complexes of SPI with five different polyphenols (TA, CGA, FA, CA, and GA) were successfully fabricated by HC treatment. The shear effect generated by HC could loosen the structure of SPI, providing more binding sites for polyphenols. At the same time, HC generated hydroxyl radicals, which could oxidize polyphenols into quinones and also oxidize amino acid residues on protein side chains, promoting the formation of C-N and C-S bonds between SPI and polyphenols, thereby allowing more polyphenols to bind to SPI. Among these five polyphenols, TA had the highest binding level with SPI and the binding level was increased by about 2 times after HC treatment, which proved that polyphenols with larger molecular weight and more hydroxyl groups were more likely to bind SPI under this condition. Additionally, a series of spectroscopy analysis further verified the effect of HC treatment on the structure of the SPI-polyphenol complexes. As expected, the antioxidant activity and emulsifying properties of SPI-polyphenols complexes formed by HC were improved, with SPI-TA exhibiting the best antioxidant activity and SPI-CA exhibiting the best EAI. Hence, HC treatment can be effectively utilized in the development of functional food proteins. The SPI-polyphenols complex prepared can be used to construct antioxidant emulsion delivery system. In the upcoming study, the prepared SPI-polyphenol complexes will be utilized for formulating an antioxidant emulsion, assessing its stability, and investigating the effect of encapsulation, delivery, and controlled release of bioactive compounds.

CRediT authorship contribution statement

Fengyan Wei: Methodology, Investigation, Data curation, Writing – original draft, Software. **Xian'e Ren:** Writing – review & editing, Methodology, Data curation, Funding acquisition. **Yongchun Huang:** Methodology, Conceptualization. **Ning Hua:** Investigation, Data curation. **Yuting Wu:** Investigation, Software. **Feng Yang:** Supervision, Conceptualization, Methodology, Writing – review & editing.

Declaration of competing interest

The authors declare that they have no known competing financial interests or personal relationships that could have appeared to influence the work reported in this paper.

Acknowledgments

The author sincerely expresses gratitude to all individuals involved in this work. The funding for this work was provided by the National Natural Science Foundation of China (no. 32360577), the Guangxi Natural Science Foundation Program (no. 2024GXNSFAA010386), and the Innovation project of Guangxi Graduate Education (no. YCSW2024519).

Data availability

Data will be made available on request.

References

- Ballon, A., Romero, M.P., Rodriguez-Saona, L.E., De Lamo-Castellví, S., Güell, C., Ferrando, M., 2024. Conjugation of lesser mealworm (*Alphitobius diaperinus*) larvae protein with polyphenols for the development of innovative antioxidant emulsifiers. *Food Chem.* 434, 137494. <https://doi.org/10.1016/j.foodchem.2023.137494>.
- Bhimrao Muley, A., Bhalchandra Pandit, A., Satishchandra Singhal, R., Govind Dalvi, S., 2020. Production of biologically active peptides by hydrolysis of whey protein isolates using hydrodynamic cavitation. *Ultrason. Sonochem.* 71, 105385. <https://doi.org/10.1016/j.ultrasonch.2020.105385>.
- Cao, Y., Xiong, Y.L., 2015. Chlorogenic acid-mediated gel formation of oxidatively stressed myofibrillar protein. *Food Chem.* 180, 235–243. <https://doi.org/10.1016/j.foodchem.2015.02.036>.
- Chen, Y., Ma, M., 2020. Foam and conformational changes of egg white as affected by ultrasonic pretreatment and phenolic binding at neutral pH. *Food Hydrocolloids* 102, 105568. <https://doi.org/10.1016/j.foodhyd.2019.105568>.
- Chen, G., Wang, S., Feng, B., Jiang, B., Miao, M., 2019. Interaction between soybean protein and tea polyphenols under high pressure. *Food Chem.* 277, 632–638. <https://doi.org/10.1016/j.foodchem.2018.11.024>.
- Chen, J., Zhang, X., Chen, X., Pius, B.A., Zhou, G., Xu, X., 2022. Phenolic modification of myofibrillar protein enhanced by ultrasound: the structure of phenol matters. *Food Chem.* 386, 132662. <https://doi.org/10.1016/j.foodchem.2022.132662>.
- Chen, Y., Li, X., Li, Q., Pan, L., Luo, J., Zha, X., 2024a. Dual decoration of quinoa protein isolate by different dietary polyphenols with covalent and noncovalent approaches: structure characterization, conformational changes and functional properties. *Food Hydrocolloids* 156, 110376. <https://doi.org/10.1016/j.foodhyd.2024.110376>.
- Chen, Y., Wei, Q., Chen, Y., Feng, A., Zhang, W., 2024b. Enhancement of hydrogen bonds between proteins and polyphenols through magnetic field treatment: structure, interfacial properties, and emulsifying properties. *Food Res. Int.* 192, 114822. <https://doi.org/10.1016/j.foodres.2024.114822>.
- Dai, L., Sun, C., Wei, Y., Mao, L., Gao, Y., 2018. Characterization of Pickering emulsion gels stabilized by zein/gum Arabic complex colloidal nanoparticles. *Food Hydrocolloids* 74, 239–248. <https://doi.org/10.1016/j.foodhyd.2017.07.040>.
- Dai, S., Xu, T., Yuan, Y., Fang, Q., Lian, Z., Tian, T., Tong, X., Jiang, L., Wang, H., 2024. Combination and precipitation mechanism of soy protein and tea polyphenols. *Food Hydrocolloids* 146, 109197. <https://doi.org/10.1016/j.foodhyd.2023.109197>.
- Dini, I., Grumetto, L., 2022. Recent advances in natural polyphenol research. *Molecules* 27 (24), 8777. <https://doi.org/10.3390/molecules27248777>.
- Fei, X., Yan, Y., Wang, L., Huang, Z., Gong, D., Zhang, G., 2023. Protocatechuic acid and gallic acid improve the emulsion and thermal stability of whey protein by covalent binding. *Food Res. Int.* 170, 113000. <https://doi.org/10.1016/j.foodres.2023.113000>.
- Geng, M., Feng, X., Yang, H., Wu, X., Li, L., Li, Y., Teng, F., 2022. Comparison of soy protein isolate-(−)-epigallocatechin gallate complexes prepared by mixing, chemical polymerization, and ultrasound treatment. *Ultrason. Sonochem.* 90, 106172. <https://doi.org/10.1016/j.ultrasonch.2022.106172>.
- Gu, L., Peng, N., Chang, C., McClements, D.J., Su, Y., Yang, Y., 2017. Fabrication of surface-active antioxidant food biopolymers: conjugation of catechin polymers to egg white proteins. *Food Biophys.* 12 (2), 198–210. <https://doi.org/10.1007/s11483-017-9476-5>.
- Han, S., Cui, F., McClements, D.J., Xu, X., Ma, C., Wang, Y., Liu, X., Liu, F., 2022. Structural characterization and evaluation of interfacial properties of pea protein isolate-EGCG molecular complexes. *Foods* 11 (18), 2895. <https://doi.org/10.3390/foods11182895>.
- Hu, W., Chen, C., Wang, Y., He, W., He, Z., Chen, J., Li, Z., Li, J., Li, W., 2023. Development of high internal phase emulsions with noncovalent crosslink of soy protein isolate and tannic acid: mechanism and application for 3D printing. *Food Chem.* 427, 136651. <https://doi.org/10.1016/j.foodchem.2023.136651>.
- Jeong, H.S., Venkatesan, J., Kim, S.K., 2013. Isolation and characterization of collagen from marine fish (*Thunnus obesus*). *Biotechnol. Bioproc. Eng.* 18 (6), 1185–1191. <https://doi.org/10.1007/s12257-013-0316-2>.
- Kang, D., Zou, Y., Cheng, Y., Xing, L., Zhou, G., Zhang, W., 2016. Effects of power ultrasound on oxidation and structure of beef proteins during curing processing. *Ultrason. Sonochem.* 33, 47–53. <https://doi.org/10.1016/j.ultrasonch.2016.04.024>.
- Ke, C., Liu, B., Dudu, O.E., Zhang, S., Meng, L., Wang, Y., Yan, T., 2023. Modification of structural and functional characteristics of casein treated with quercetin via two interaction modes: covalent and non-covalent interactions. *Food Hydrocolloids* 137, 108394. <https://doi.org/10.1016/j.foodhyd.2022.108394>.
- Kim, W., Wang, Y., Selomulya, C., 2024. Emerging technologies to improve plant protein functionality with protein-polyphenol interactions. *Trends Food Sci. Technol.* 147, 104469. <https://doi.org/10.1016/j.tifs.2024.104469>, 2024.
- Li, Y., Zhang, Z., Ren, W., Wang, Y., Mintah, B.K., Dabbour, M., Hou, Y., He, R., Cheng, Y., Ma, H., 2021b. Inhibition effect of ultrasound on the formation of lysinoalanine in rapeseed protein isolates during pH shift treatment. *J. Agric. Food Chem.* 69 (30), 8536–8545. <https://doi.org/10.1021/acs.jafc.1c02422>.
- Li, X., Dai, T., Hu, P., Zhang, C., Chen, J., Liu, C., Li, T., 2020a. Characterization the non-covalent interactions between beta lactoglobulin and selected phenolic acids. *Food Hydrocolloids* 105, 105761. <https://doi.org/10.1016/j.foodhyd.2020.105761>.
- Li, Y., He, D., Li, B., Lund, M.N., Xing, Y., Wang, Y., Li, F., Cao, X., Liu, Y., Chen, X., Yu, J., Zhu, J., Zhang, M., Wang, Q., Zhang, Y., Li, B., Wang, J., Xing, X., Li, L., 2021c. Engineering polyphenols with biological functions via polyphenol-protein interactions as additives for functional foods. *Trends Food Sci. Technol.* 110, 470–482. <https://doi.org/10.1016/j.tifs.2021.02.009>.
- Li, X., Li, M., Zhang, T., McClements, D.J., Liu, X., Wu, X., Liu, F., 2021a. Enzymatic and nonenzymatic conjugates of lactoferrin and (−)-Epigallocatechin gallate: formation, structure, functionality, and allergenicity. *J. Agric. Food Chem.* 69 (22), 6291–6302. <https://doi.org/10.1021/acs.jafc.1c01167>.
- Li, D., Zhao, Y., Wang, X., Tang, H., Wu, N., Wu, F., Yu, D., Elfalleh, W., 2020b. Effects of (+)-catechin on a rice bran protein oil-in-water emulsion: droplet size, zeta-potential, emulsifying properties, and rheological behavior. *Food Hydrocolloids* 98, 105306. <https://doi.org/10.1016/j.foodhyd.2019.105306>.
- Li, D., Zhu, L., Wu, Q., Chen, Y., Wu, G., Zhang, H., 2023. Identification of binding sites for Tartary buckwheat protein-phenols covalent complex and alterations in protein structure and antioxidant properties. *Int. J. Biol. Macromol.* 233, 123436. <https://doi.org/10.1016/j.ijbiomac.2023.123436>.
- Liao, Y., Kang, M., Kou, T., Yan, S., Chen, T., Gao, Y., Qi, B., Li, Y., 2024. Effects of three polyphenols with different numbers of phenolic hydroxyls on the structural and interfacial properties and lipid-protein co-oxidation of oil body emulsions. *Food Hydrocolloids* 154, 110077. <https://doi.org/10.1016/j.foodhyd.2024.110077>.
- Liu, X., Xue, F., Adhikari, B., 2023. Production of hemp protein isolate-polyphenol conjugates through ultrasound and alkali treatment methods and their characterization. *Future Foods* 7, 100210. <https://doi.org/10.1016/j.fufo.2022.100210>.
- Liu, J., Song, G., Zhou, L., Yuan, Y., Wang, D., Yuan, T., Li, L., He, G., Xiao, G., Chen, F., Gong, J., 2023a. Sonochemical effects on fabrication, characterization and antioxidant activities of β -lactoglobulin-chlorogenic acid conjugates. *Ultrason. Sonochem.* 92, 106240. <https://doi.org/10.1016/j.ultrasonch.2022.106240>.
- Liu, J., Song, G., Zhou, L., Yuan, Y., Wang, D., Yuan, T., Li, L., Yuan, H., Xiao, G., Gong, J., 2023b. Recent advances in the effect of ultrasound on the binding of protein–polyphenol complexes in foodstuff. *Food Frontiers* 4 (2), 721–732. <https://doi.org/10.1002/fft2.221>.
- Liu, J., Zhang, Y., Liu, J., Zhang, H., Gong, L., Li, Z., Liu, H., Wang, Z., 2024. Effect of non-covalently bound polyphenols on the structural and functional properties of wheat germ protein. *Food Hydrocolloids* 149, 109534. <https://doi.org/10.1016/j.foodhyd.2023.109534>.
- Meng, Y., Li, C., 2021. Conformational changes and functional properties of whey protein isolate-polyphenol complexes formed by non-covalent interaction. *Food Chem.* 364, 129622. <https://doi.org/10.1016/j.foodchem.2021.129622>.
- Mohammadi, A., Kashi, P.A., Kashiri, M., Bagheri, A., Chen, J., Ettelaie, R., Shahbazi, M., 2023. Self-assembly of plant polyphenols-grafted soy proteins to manufacture a highly stable antioxidative Pickering emulsion gel for direct-ink-write 3D printing. *Food Hydrocolloids* 142, 108851. <https://doi.org/10.1016/j.foodhyd.2023.108851>.
- Pan, L., Chen, J., Fu, H., Wang, N., Zhou, J., Zhang, S., Lu, S., Dong, J., Wang, Q., Yan, H., 2023. Effects of fabrication of conjugates between different polyphenols and bovine bone proteins on their structural and functional properties. *Food Biosci.* 52, 102375. <https://doi.org/10.1016/j.fbio.2023.102375>.
- Panda, D., Saharan, V.K., Manickam, S., 2020. Controlled hydrodynamic cavitation: a review of recent advances and perspectives for greener processing. *Processes* 8 (2), 220. <https://doi.org/10.3390/pr8020220>.
- Parolia, S., Maley, J., Sammynaiken, R., Green, R., Nickerson, M., Ghosh, S., 2022. Structure – functionality of lentil protein-polyphenol conjugates. *Food Chem.* 367, 130603. <https://doi.org/10.1016/j.foodchem.2021.130603>.
- Patil, C., Sonawane, S., Bhalerao, P., Dabade, A., 2023. The effect of non-thermal hydrodynamic cavitation process on structural and function properties of casein

- protein. *Journal of Agriculture and Food Research* 14, 100899. <https://doi.org/10.1016/j.jafr.2023.100899>.
- Pi, X., Sun, Y., Liu, J., Wang, X., Hong, W., Cheng, J., Guo, M., 2023. Characterization of the improved functionality in soybean protein-proanthocyanidins conjugates prepared by the alkali treatment. *Food Hydrocolloids* 134, 108107. <https://doi.org/10.1016/j.foodhyd.2022.108107>.
- Ren, X., Li, C., Yang, F., Huang, Y., Huang, C., Zhang, K., Yan, L., 2020. Comparison of hydrodynamic and ultrasonic cavitation effects on soy protein isolate functionality. *J. Food Eng.* 265, 109697. <https://doi.org/10.1016/j.jfoodeng.2019.109697>.
- Sun, J., Liu, T., Zhang, F., Huang, Y., Zhang, Y., Xu, B., 2022. Tea polyphenols on emulsifying and antioxidant properties of egg white protein at acidic and neutral pH conditions. *LWT - Food Sci. Technol. (Lebensmittel-Wissenschaft -Technol.)* 153, 112537. <https://doi.org/10.1016/j.lwt.2021.112537>.
- Tian, L., Kejing, Y., Zhang, S., Yi, J., Zhu, Z., Decker, E.A., McClements, D.J., 2021. Impact of tea polyphenols on the stability of oil-in-water emulsions coated by whey proteins. *Journal of Food Chemistry* 343, 128448. <https://doi.org/10.1016/j.foodchem.2020.128448>.
- Wang, T., Chen, X., Wang, W., Wang, L., Jiang, L., Yu, D., Xie, F., 2021a. Effect of ultrasound on the properties of rice bran protein and its chlorogenic acid complex. *Ultrason. Sonochem.* 79, 105758. <https://doi.org/10.1016/j.ultsonch.2021.105758>.
- Wang, D., Li, H., Hou, T.Y., Zhang, Z.J., Li, H.Z., 2024. Effects of conjugated interactions between Perilla seed meal proteins and different polyphenols on the structural and functional properties of proteins. *Food Chem.* 433, 137345. <https://doi.org/10.1016/j.foodchem.2023.137345>.
- Wang, Q., Tang, Y., Yang, Y., Lei, L., Zhao, J., Zhang, Y., Li, L., Wang, Q., Ming, J., 2021b. Combined effects of quercetin and sodium chloride concentrations on wheat gliadin structure and physicochemical properties. *J. Sci. Food Agric.* 101 (6), 2511–2518. <https://doi.org/10.1002/jsfa.10877>.
- Wen, C., Liu, G., Ren, J., Deng, Q., Xu, X., Zhang, J., 2022. Current progress in the extraction, functional properties, interaction with polyphenols, and application of legume protein. *J. Agric. Food Chem.* 70 (4), 992–1002. <https://doi.org/10.1021/acs.jafc.1c07576>.
- Xie, K., Yang, F., Ren, X., Huang, Y., Wei, F., 2024. Insight into the effects of hydrodynamic cavitation at different ionic strengths on physicochemical and gel properties of myofibrillar protein from Tilapia (*Oreochromis niloticus*). *Foods* 13 (6), 851. <https://doi.org/10.3390/foods13060851>.
- Yan, S., Xie, F., Zhang, S., Jiang, L., Qi, B., Li, Y., 2021. Effects of soybean protein isolate – polyphenol conjugate formation on the protein structure and emulsifying properties: protein – polyphenol emulsification performance in the presence of chitosan. *Colloids Surf. A Physicochem. Eng. Asp.* 609, 125641. <https://doi.org/10.1016/j.colsurfa.2020.125641>.
- Yang, F., Liu, X., Ren, X., Huang, Y., Huang, C., Zhang, K., 2018. Swirling cavitation improves the emulsifying properties of commercial soy protein isolate. *Ultrason. Sonochem.* 42, 471–481. <https://doi.org/10.1016/j.ultsonch.2017.12.014>.
- Yu, J., Xie, S., Yang, D., 2024. The changes induced by hydrodynamic cavitation treatment in wheat gliadin and celiac-toxic peptides. *J. Food Sci. Technol.* 61 (10), 1976–1985. <https://doi.org/10.1007/s13197-024-05973-7>.
- Zhang, Z., Wang, Y., Jiang, H., Dai, C., Xing, Z., Kumah Mintah, B., Dabbour, M., He, R., Ma, H., 2020. Effect of dual-frequency ultrasound on the formation of lysinoalanine and structural characterization of rice dreg protein isolates. *Ultrason. Sonochem.* 67, 105124. <https://doi.org/10.1016/j.ultsonch.2020.105124>.
- Zhang, Y., Wu, C., Shen, X., McClements, D.J., Liu, X., Liu, F., 2025. Effects of combined hot alkaline and pH-shift treatments on structure and functionality of legume protein-EGCG conjugates: soybean-, pea-, and chickpea protein-EGCG systems. *Food Hydrocolloids* 158, 110424. <https://doi.org/10.1016/j.foodhyd.2024.110424>.
- Zheng, Y., Chen, B., Huang, X., Teng, H., Ai, C., Chen, L., 2023. Ultrasound-assisted free radical modification on the structural and functional properties of ovalbumin-epigallocatechin gallate (EGCG) conjugates. *Ultrason. Sonochem.* 95, 106396. <https://doi.org/10.1016/j.ultsonch.2023.106396>.
- Zhou, S.D., Lin, Y.F., Xu, X., Meng, L., Dong, M.S., 2020. Effect of non-covalent and covalent complexation of (–)-epigallocatechin gallate with soybean protein isolate on protein structure and in vitro digestion characteristics. *Food Chem.* 309, 125718. <https://doi.org/10.1016/j.foodchem.2019.125718>.